R-2362

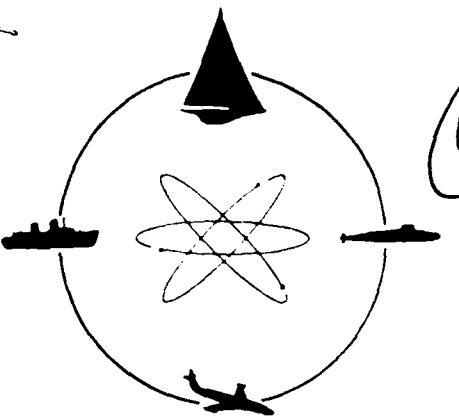

(12)

DAVIDSON LABORATORY

Report SIT-DL-83-9-2362
August 1983

MODEL TEST OF A WATERJET PROPULSION SYSTEM FOR HIGH SPEED AMPHIBIANS

by

F. Thomas Korsmeyer

APPROVED FOR PUBLIC RELEASE:
DISTRIBUTION UNLIMITED

ENS INSTITUTE
TECHNOLOGY

E POINT STATION
N, NEW JERSEY 07030

R-2362

SECURITY CLASSIFICATION OF THIS PAGE (When Data Entered)

REPORT DOCUMENTATION PAGE

READ INSTRUCTIONS BEFORE COMPLETING FORM

1. REPORT NUMBER: SIT-DL-83-9-2362	2. GOVT ACCESSION NO.: AD-A140 352
3. RECIPIENT'S CATALOG NUMBER:	
4. TITLE (and Subtitle): MODEL TEST OF A WATERJET PROPULSION SYSTEM FOR HIGH SPEED AMPHIBIANS.	5. TYPE OF REPORT & PERIOD COVERED: FINAL REPORT
	6. PERFORMING ORG. REPORT NUMBER: Davidson Laboratory R-2362
7. AUTHOR(s): F. Thomas Korsmeyer	8. CONTRACT OR GRANT NUMBER(s): N00167-82-K-0114.
9. PERFORMING ORGANIZATION NAME AND ADDRESS: Davidson Laboratory, STEVENS INSTITUTE OF TECHNOLOGY, Castle Point Station, Hoboken, NJ 07030	10. PROGRAM ELEMENT, PROJECT, TASK AREA & WORK UNIT NUMBERS:
11. CONTROLLING OFFICE NAME AND ADDRESS: David W. Taylor Naval Research and Development Center (Code 112), Bethesda, MD 20362	12. REPORT DATE: August 1983
	13. NUMBER OF PAGES: vi + 19 pp.+ 7 tables+ 6 figures.
14. MONITORING AGENCY NAME & ADDRESS (if different from Controlling Office)	15. SECURITY CLASS. (of this report):
	15a. DECLASSIFICATION/DOWNGRADING SCHEDULE:

16. DISTRIBUTION STATEMENT (of this Report)

APPROVED FOR PUBLIC RELEASE: DISTRIBUTION UNLIMITED

17. DISTRIBUTION STATEMENT (of the abstract entered in Block 20, if different from Report)

18. SUPPLEMENTARY NOTES

19. KEY WORDS (Continue on reverse side if necessary and identify by block number)

WATERJET
PROPULSION
MODEL TEST

20. ABSTRACT (Continue on reverse side if necessary and identify by block number)

A simple, bottom-inlet, waterjet was designed for evaluation in a fifteen-foot, manned testcraft. To aid in the planning of the experiments to be conducted with this craft, a 1/4.828 scale model was built and tank tested. The impeller was a stock 4-bladed marine model propeller housed in a cylindrical duct. Model resistance and trim were measured over a range of speeds. Waterjet velocity; propeller thrust, torque and rpm; and static pressures in the inlet casing were measured at several speeds bracketing the drag hump. Model waterjet performance was compared to design predictions.

DD FORM 1 JAN 73 1473 EDITION OF 1 NOV 65 IS OBSOLETE
S/N 0102-014-6601

SECURITY CLASSIFICATION OF THIS PAGE (When Data Entered)

STEVENS INSTITUTE OF TECHNOLOGY
DAVIDSON LABORATORY
Castle Point Station, Hoboken, New Jersey 07030

Report SIT-DL-83-9-2362

August 1983

MODEL TEST OF A WATERJET PROPULSION SYSTEM FOR HIGH SPEED AMPHIBIANS

by

F. Thomas Korsmeyer

APPROVED FOR PUBLIC RELEASE:
DISTRIBUTION UNLIMITED

Prepared for

Code 112
David W. Taylor
Naval Ship Research and Development Center
Under

Contract Number N00167-82-K-0114
(DL Project 5052/220)

APPROVED:

Daniel Savitsky
Acting Director

TABLE OF CONTENTS

LIST OF TABLES

LIST OF FIGURES

NOMENCLATURE

A_j	Jet area, ft^2
D_D	Duct diameter in way of propeller, ft
D_P	Propeller diameter, ft
D_{bare}	Bare hull drag, lbs
D_{ext}	Drag of the hull with the propulsion system operating, lbs
D_m	Drag measured during the powered test, lbs
f	Friction factor
F_{cv}	Forces in the control volume on the boundaries, lbs
F_p	Forces due to pressure on the entrance and exit planes of the control volumes, lbs
F_w	Friction and pressure forces on the duct walls, struts, shaft, lbs
g	Acceleration due to gravity, 32.174 ft/s^2
H	Head induced by the propeller, ft , $T/\gamma A_j$
J_D	Advance ratio based on the duct flow, V_j/nD_P
J_{fs}	Advance ratio based on the free stream V_m/nD_P
K_H	Head coefficient, $gH/n^2D_D^2$
K_Q	Torque coefficient, $Q/\rho n^2D_P^5$
$K_{\bar{Q}}$	Flow coefficient, $\bar{Q}/nD_D^3$
K_T	Thrust coefficient, $T/\rho n^2D_P^4$
L	Loss, ft
n	Shaft revolutions per second
P/D	Pitch-diameter ratio
P_i	Inlet static pressure, lbs/ft^2
P_j	Jet static pressure, lbs/ft^2
P_D	Jet dynamic pressure, lbs/ft^2
$P_{0.7}$	Jet static pressures measured at 0.7 radius, top dead center, lbs/ft^2

Q	Torque, lbs-ft
$\bar{Q}$	Flow rate, ft^3/sec
T	Shaft thrust, lbs
T_{gr}	Gross thrust, lbs, $\rho\bar{Q}(\beta_j V_j - V_m)$
T_{net}	Net thrust, lbs, $D_m - D_{bare}$
$(1 - t)$	Thrust deduction factor, $\frac{D_{bare}}{D_m - T_{gr}\cos\tau}$
V_i	Inlet velocity, ft/sec
V_j	Jet velocity, ft/sec
V_m	Model velocity, ft/sec
V_o	Entrance velocity, ft/sec
V_s	Manned test craft velocity, ft/sec
$V_{0.7}$	Velocity at the 0.7 radius, top dead center, ft/sec
w_s	Shaft work, (equals H), ft
z	Heave at LCG, ft
β_i, β_j	Velocity distribution factors
Δ	Static displacement, lbs
γ	Density times g , lbs/ft^3
ρ	Density, 1.94 $slugs/ft^3$
η_{oa}	Overall efficiency, $T_{net} V_m/2\pi Qn$
η_{pump}	Pump efficiency, $\gamma\bar{Q}H/2\pi Qn$
η_{prop}	Propulsion efficiency, $\eta_{pump} V_m/V_j$
τ	Trim angle, baseline relative to calm free surface, deg
τ_{bare}	Trim during EHP test, deg

INTRODUCTION

A simple, bottom-inlet, waterjet was designed for evaluation in a fifteen-foot, manned testcraft. To aid in the planning of the experiments to be conducted with this craft, a 1/4.828 scale model was built and tested at Davidson Laboratory in May 1983. This work was performed under Office of Naval Research Contract N00167-82-K-0114; technical monitoring was provided by Mr. W. Zeitfuss, Jr., Code 112, David W. Taylor Naval Ship Research and Development Center. A portion of the model test was witnessed by Mr. Zeitfuss and Mr. John Hoyt.

The goals of the model experiment were to determine the resistance of the manned testcraft, to characterize the model propulsion system, and to use this characterization to reflect on the merits of the waterjet design method used for the manned testcraft. This method was developed with Mr. John K. Roper, and is detailed in Reference 5.

TEST PROGRAM

The bare hull resistance portion of the test had two purposes. The first was to provide EHP curves for the manned testcraft, and the second was to have the bare hull drag value needed to define thrust deduction for the model. The powered portion of the test involved the measurement of shaft torque and thrust as well as pressures and velocities in the waterjet. These measurements were used to find efficiencies and to quantify some of the losses in the system.

THE MODEL

A scale ratio of 1:4.828 was chosen so that a stock Davidson Laboratory propeller could be used. The model hull was constructed of clear acrylic sheet, fastened with a solvent-type cement. The duct was constructed of glass fiber reinforced plastic, layed up on a wooden, male form. This was bolted into the model against a hole cut in the model bottom and one cut in the aft end of the *pump box*. (See schematic, Figure 1.) Exterior to the pump box a copper nozzle was fitted which housed the propeller and carried the shaft bearing on a cruciform strut. The shaftline was set at 2 degrees relative to the baseline to allow sufficient clearance for the drive motor dynamometry. Model particulars are listed in Table 1.

Two aspects of the model were dictated by the fact that it was designed as representative of a tracked amphibian. One feature was the 2 degree wedge placed on the bottom, just aft of the transom, for some of the testing. This simulated the bottom contour possible with a hinged tailgate. The other feature was the free-flooding track covers which extended along each side of the model, providing a flat bottom out to the maximum beam. The spaces enclosed by the track covers emptied from the open aft end when the model was run at planing speeds.

The model was attached to the towing carriage by a free to heave and trim system which connected to the model on the shaftline. Movable ballast provided the two load conditions shown in Table 1.

THE INSTRUMENTATION

For the EHP portion of the testing, the model was instrumented with transducers for measuring drag, heave and trim:

Drag. A spring and differential transformer force-block was mounted above the pitch pivot so that drag was measured parallel to the free surface.

Heave. A rotary, variable differential transformer was affixed to the carriage, and sensed vertical motion of the pitch pivot point through a string connection.

Trim. An accelerometer-type inclinometer was mounted on the model and sensed trim angles relative to the calm free surface.

For the powered test, there were additional transducers for shaft torque, thrust and speed, and for pressures in the duct and jet.

Torque and Thrust. The propulsion motor was cradled in a spring and differential transformer system which sensed the reaction of the stator to the load on the armature.

Shaft Speed. The shaft was fitted with a ten-toothed gear-like wheel which excited a magnetic pickup. A pulse counter detected the signal and averaged it in one-second intervals.

Static Pressure. Water-filled pressure taps and tubes were set into the duct wall and connected to diaphram-type pressure gages. The taps were located as shown in Figure 2.

Jet Velocity. The jet velocity was derived from dynamic head measured with a Prandtl tube which could be moved in the nozzle exit plane. The static and total head orifices were connected by water-filled tubes to diaphram-type pressure gages.

In all of the testing, carriage speed was measured by an optical system which sensed the carriage travel during the elapsed time of the data collection portion of each test run.

The precision of these instruments is judged to be approximately 1% of full scale or better, and each was selected and calibrated so that the

measured values exceeded 50% of full scale during most of the testing. The wetted length of the model bottom and the area wetted by reattached flow was visually estimated from the videotape record of the test with the aid of one-inch markings along the chine. The precision of this measurement is judged to be ±½ inch, which results in ±3% of wetted area at planing speeds.

The signals from the transducer were relayed during each test run via overhead cables to the onshore data acquisition and recording equipment. With the exception of shaft speed, each data channel was digitally averaged by the hardware and software of a PDP8-e Computer, converted to engineering units and reported on a computer terminal. Shaft speed was read during each run by tank personnel from a digital readout with a 1/10 RPS resolution. Computer files of data were later relayed to the Stevens Institute of Technology DEC-10 system for analysis.

PROCEDURE

The model testing was conducted in Davidson Laboratory Tank 3 (313' x 12' x 5.5'(depth)). In the heavy load condition, the pitch pivot (towpoint) was at the intersection of the shaftline and the transverse plane of the LCG. In the light load condition, the transverse plane of the LCG was 0.37 inches aft of the pitch pivot.

For EHP testing, the entrance and exit to the duct were blocked off with 1/16" thick sheets of fiberglas reinforced plastic which provided a flat bottom in way of the duct entrance, and kept the duct completely full of water. There was no form of turbulence stimulation.

The procedure for EHP testing was as follows:

1) Zero values for drag and heave were recorded with the model at rest. The trim zero was set to be equal to a condition of the model baseline (keel) parallel to the calm free surface.

2) The model weight was unloaded at the pivot point by an amount equal to the vertical component of the thrust required for equilibrium at the speed to be run. This is, of course, an estimated value:

   Unload = Estimated Drag x sine(Estimated Trim + Shaft Angle) .

   If the run results indicated that the unloading weight was

incorrect by more than 10% of the correct value, the run was repeated.

3) The model was accelerated by the towing carriage to the desired speed, and after steady-state conditions were established, data were recorded for 50 feet of model travel.

4) Approximately 4 minutes were allowed to pass before a succeeding run, to quiet the tank surface.

The procedure in the powered testing was as follows:

1) With the model at rest, zero values were recorded as above. In the case of pressure transducers the recorded zeros contained a head of water equal to the submergence of the taps. These were subtracted later. Torque and thrust zeros were taken with the shaft stationary.

2) The model and propeller shaft were accelerated to the desired speeds, and after steady-state conditions were established, data were recorded for 40 feet of model travel.

3) Approximately 4 minutes were allowed to pass before a succeeding run, to quiet the tank surface.

The EHP testing was conducted over a speed range sufficient to define the resistance hump as well as up to approximately 26 feet/second as a practical top speed. This was done for a light load, 40.0 pounds, and a heavy load, 49.5 pounds, and also in the heavy load condition with the 2 degree wedge added (see Figure 1).

The powered testing was conducted primarily at two speeds: 8.01 and 9.34 feet/second. At 8.01 feet/second, the testing was extensive, and included a velocity survey of the jet. In the initial testing at 8.01 feet/second and 9.34 feet/second, shaft speed was varied so that waterjet performance could be quantified over a range of propeller advance ratios. In the wake survey (at 8.01 ft/sec), model speed and shaft speed were held constant for repeated runs while the Prandtl tube was moved to different locations in the jet, and set at various angles away from axial alignment.

DATA ANALYSIS AND RESULTS

EHP TEST

Effective horsepower results were expanded to the manned testcraft scale using the ATTC friction line. Wetted area was calculated from the observed wetted lengths and the observed reattached flow on the model sides when it was present. The results of this expansion are for fresh water at 59°F and do not include a roughness allowance. These results are presented for the light load and heavy load, with and without the 2 degree wedge, in Tables 2, 3, and 4, and in Figures 3 and 4.

The model scale resistance results were used in the powered test data analysis to determine a thrust deduction factor.

POWERED TEST

General

The powered test was conducted to define the waterjet performance and its effects on the vehicle. The test was largely confined to three conditions, all at the heavy load: 8.01 ft/sec with and without the 2 degree wedge, and 9.34 ft/sec without the 2 degree wedge. Two runs were also made at higher speeds, 14.01 and 15.35 ft/sec, without the wedge. While model speed was held constant, the shaft speed was varied so that a range of operating conditions was spanned, from where the propeller was blocking the duct flow, to where the model was nearly self-propelled.

The data were analyzed with the help of a computer program which produced the output listed in Tables 5 through 7. Tables 5 and 6 give measured values and some of those values in more useful coefficient form. Table 7 presents an analysis which probes more deeply into the nature of beneficial and adverse efforts of the waterjet on the vehicle, and defines the energy losses in the waterjet flow.

In Table 5, the measured data are presented in dimensional form, in the slugs-feet-second system. All of these are primary, measured quantities except the jet velocity, V_j, and the flow rate, $\bar{Q}$, which were found

by a dynamic pressure measurement and a calculation described below. The last two columns in Table 5 simply restate the bare hull drag and trim values found in the EHP test for useful comparison to gross thrust, T_{gr}, and because these values are involved in the calculation of the net thrust, T_{net}, and the thrust deduction, (1-t). The two listed pressures: in the jet, P_j, and in the inlet plane, P_i, are static pressures relative to the atmosphere.

In Table 6, the measured values have been combined with each other and some system geometry to produce a series of coefficients and efficiencies which are common to pump analysis and to powered vehicle analysis. Vehicle and propeller-oriented coefficients, J, K_T, K_Q, were non-dimensionalized on the propeller diameter, D_P, and the waterjet-oriented coefficients were non-dimensionalized on the duct diameter, D_D. The difference between the two is slight — just the tip clearance — but it becomes significant at the high powers of D involved in the denominators of these coefficients. Consequently, the efficiencies are not calculated as ratios of the coefficients, but rather as the ratios of the various dimensional quantities of *power-in* and *power-out*.

The two coefficients which concern the waterjet performance alone are the flow coefficients, $K_{\bar{Q}}$, and the head coefficient K_H. η_{pump} relates the head and flow (not the coefficients) in the usual form of hydraulic work, $\gamma\bar{Q}H$, to the input horsepower. η_{prop} is the pump efficiency multiplied by the ratio, V_m/V_j. This value always decreases as thrust increases and simply reflects the fact, also common to usual ship propulsion analysis, that increased propulsor diameter can increase thrust by increasing $\bar{Q}$ without increasing V_j and decreasing efficiency.

Two coefficients combine waterjet and vehicle performance: the thrust deduction (1-t) and the overall efficiency, η_{oa}. The addition of the waterjet to the bare hull condition adds a considerable drag in the form of adverse pressures on the ramp, but offsetting this is the beneficial effect which this propulsion system has on running trim. That is, both drag increases and drag reductions are found in (1-t). This is discussed in detail in the "Momentum Analysis" section. η_{oa} has similar characteristics because it is the ratio of net power-out to power-in,

that is,

$$\eta_{oa} = \frac{T_{net} V_m}{2\pi Q n} \quad ,$$

so this value, too, contains interactions between the vehicle and the propulsion system.

Table 7 is an attempt to break down the forces and energy losses in the waterjet. This analysis has been done on the basis of an analysis of the flow through two control volumes. Figure 2 shows the boundaries of the two control volumes. Number One is bounded by an entrance surface and the stagnation stream surface; it extends into the duct entrance to be bounded by the duct ramp, and has an exit plane which is designated the duct inlet plane. Number Two has the duct inlet as its entrance plane, and continues, bounded by the duct walls to the nozzle exit plane.

Knowledge of the flow conditions at these exit and entrance planes is critical to finding the forces on the fluid, the gross thrust of the system, and the losses through the duct. Measurements were made to quantify these flow conditions, but it was not practical to thoroughly define all of them at each operating condition. The following discussion describes the assumptions and approximations which were used at various portions of the control surfaces:

Exit Plane, Control Volume Two. Static and dynamic pressure were measured at the 0.7 radius, top dead center, during every run, and a wake survey was conducted at the one operating condition of 8.01 ft/sec model speed, and 87.5 rev/sec shaft speed. It was assumed that the velocity and pressure at the 0.7 radius were related to the average velocity, the momentum, and the average pressure by the same constant factors at all operating conditions as was found at the survey condition. How these factors were found is explained in the section on the wake survey.

Entrance Plane, Control Volume Two, Exit Plane Control Volume One. The flow rate here was found by continuity from the jet flow rate. The non-uniformity of the velocity distribution was assumed to be one-half that found in the survey of the jet. The static pressure was found by averaging the two static pressure measurements made in this plane.

Entrance Plane, Control Volume One. This plane was located ahead of the ramp and perpendicular to the model bottom. It was assumed that the plane was no wider than the entrance to the duct. The total energy in the flow through this plane was assumed to be equal to the free stream energy upstream of the model. This was calculated by extending the stagnation streamsurface upstream, by continuity and the two-dimensional flow assumption, to where the velocity could be taken as V_m

and the pressure as hydrostatic at the center of the flow cross sectional area. At the entrance plane, this total energy was apportioned between head and flow by the assumption that the local velocity was reduced by the presence of the boundary layer and the inception of planing (as evidenced by positive heave values) to 0.9 V_m . The forces on the stagnation stream surface were assumed to be negligible.

With these assumptions and approximations, and with the measured forces on the model, it was possible to examine the performance of the waterjet and model through the use of the momentum equation, a force balance on the model, and the energy equation.

Wake Survey Details

The purpose of the survey was to find the velocity distribution throughout the cross-section of the jet, where the magnitude would be used to find flow rate, $\bar{Q}$, and gross thrust, T_{gr} , and the direction would be used to help in stator design. Since a Prandtl tube was used in this survey, the flow direction was not measured at every survey point. Rather, at one point, the 0.7 radius at 0° (top dead center), the magnitudes of the static, dynamic, and total pressures were recorded as the axis of the tube was rotated to either side, away from alignment with the axis of the jet. Prandtl has shown that the pitot tube of his design is remarkably insensitive to alignment with the flow up to deviations of as much as 20 degrees. However, beyond this orientation, the measured dynamic and total pressures will be substantially less than the true values. Using this information, the tangential component of the flow can be estimated.

Figure 5 shows a plot of the static, dynamic, and total pressures plotted against the angle (in the approximately horizontal plane) between the Prandtl tube and jet axes. The plot is similar to that given by Prandtl,[2] and indicates that an alignment angle of 9 degrees is midway between the shoulders of the pressure curves and is therefore the point where the tube axis is parallel to the vector sum of the axial and tangential components of the flow. This 9-degree-deviation from purely axial flow is in a clockwise sense, which is consistent with the rotation of a right-hand propeller. This information may be useful in stator design, but since the cosine of 9 degrees is 0.99, the information was not used to modify momentum calculations.

The velocity survey covered 18 points on the 0° to 180° diagonal and the 90° to 270° diagonal as shown in Figure 6. The static pressure

measurement was removed from the total pressure measurement, and the magnitude of the velocity was found from $V = \sqrt{2P_D/\rho}$. To minimize uncertainties in the analysis, the measured pressures in the jet were converted to two different velocity averages. This consideration arises from the fact that in calculating the forces on a control volume from the momentum flux, the basic equation from Reference 4 is

$$\sum \vec{F} = \frac{\partial}{\partial t} \int_{cv} \rho \vec{V} \, dV + \int_{cs} \rho \vec{V} \cdot \vec{V} \, dA$$

which when the time rate of change of momentum within the control volume is neglected, and when we assume a uniform velocity distribution across the control surface, we often approximate as

$$\sum F = \rho \bar{Q} \left(V_{out} - V_{in}\right) \quad .$$

However, since the jet velocity distribution is not uniform and is known, the best use of the data suggests an approximation which uses the mean of the squares instead of the square of the mean. Therefore, the dynamic pressure measured by the Prandtl tube was used to calculate velocity averages in two ways, both ways working from a faired plot of pressure versus location:

1) Faired dynamic pressure values were read in 0.1 radius increments across the two diameters. These were converted to squared velocity values and summed by Simpson's Rule over the jet area to get $(V^2)_j$.

2) Faired dynamic pressure values were again read across the two diameters and converted to velocity values. These were summed by Simpson's Rule to get V_j and $\bar{Q}$.

$(V^2)_j$ and V_j were found for other operating conditions by assuming that the relation between the velocity at the 0.7 radius, 0^o, and V_j did not change with model or shaft speed, and that the relation between $(V^2)_j$ and $(V_j)^2$ also did not change. Hence in all operating conditions other than model speed of 8.01 ft/sec and shaft speed of 87.5 rev/sec, the performance of the waterjet was estimated with the aid of the relations:

$$V_j = 0.812 \, V_{0.7}$$

$$(V^2)_j = 1.092 (V_j)^2 \, ,$$

and

$$(V^2)_i = 1.046 (V_i)^2 \, .$$

The static pressure measurements also required estimation. Like velocity, the static pressure distribution across the exit plane was assumed at all operating conditions to be like the survey condition; the relation used was:

$$P_j = 0.75\, P_{0.7} \quad .$$

MOMENTUM ANALYSIS AND FORCE BALANCE

The momentum equation was used to find the forces of the fluid in the duct on the duct walls, which is an aid in quantifying the difference between the gross and net thrusts. The nomenclature and technique used in this analysis are adopted from Etter and Scherer.[3] In all of the force-oriented analysis, it must be remembered that the waterjet is operating in a vehicle, the drag of which is greatly influenced by the flow conditions in the jet.

The two momentum equations for the two control volumes are:

$$\sum F_{cv1} = \rho \bar{Q} (\beta_i V_i - V_o)$$

and

$$\sum F_{cv2} = \rho \bar{Q} (\beta_j V_j - \beta_i V_i)$$

where it is understood that these are linear momentum equations, written parallel to the vehicle baseline, and that forces with positive magnitudes contribute to thrust, and forces with negative magnitudes contribute to drag. On the left-hand sides of these equations, the sums of the forces include:

$$\text{Wall Friction + Wall Pressure + Shaft Friction + Entrance and Exit Pressures} = \sum F_{cv1}$$

$$\text{Wall Friction + Wall Pressure + Shaft and Strut Friction + Propeller Thrust + Entrance and Exit Pressures} = \sum F_{cv2}$$

With the assumptions made above, and the model test data, the only unknowns are the aggregate wall pressure and surface friction forces. The momentum through the two control volumes is calculated, $\sum F_{cv1}$ and $\sum F_{cv2}$, then F_{p1} and F_{p2}, the pressure forces on the entrance and exit planes, are subtracted. These values and their differences F_{w1} and F_{w2} are listed in Table 7.

F_{w1} is usually negative due to the less-than-atmospheric pressure on the ramp which induces a drag component force. F_{w2} is usually positive because flow acceleration results in pressure reduction in the transition portion of CV2 between the rectangular inlet plane and the cylindrical duct, Figure 2. The pressure reduction induces a thrust component force on the curved lower wall of the transition.

F_{w1} generally becomes less negative with increasing flow rate at any model speed, which is not expected and points to uncertainty in this analysis. The initial V_o and P_o, and final V_j and P_j, are known with confidence, while the P_i measurement, being the average of only two readings, is not known with as much confidence. Therefore, the total $(F_{w1}+F_{w2})$ is more likely to be reliable than either portion alone.

To analyze the effect of the duct system on the vehicle, an equilibrium equation in the direction of model travel can be written for the forces on the model:

$$0 = D_{ext} - D_m + \left(F_{cv1} + F_{cv2}\right)\cos\tau$$

where D_m is the measured drag, and D_{ext} is by definition the drag of the vehicle with the waterjet operating. The gross thrust is defined as:

$$T_{gr} = \rho\bar{Q}\left(\beta_j V_j - V_m\right) ,$$

and the net thrust is defined as:

$$T_{net} = D_m - D_{bare}$$

where D_{bare} is the model drag without the waterjet, that is, from the EHP test. In the conventional powering sense the thrust deduction is:

$$(1-t) = \frac{D_{bare}}{D_m - T_{gr}\cos\tau}$$

and like the difference between T_{gr} and T_{net}, (1-t) encompasses all of the changes in vehicle drag due to the operation of the waterjet. The inlet drag could cause low values of (1-t), but the reduction of vehicle drag due to the change in trim largely offsets this. Since planing boat drag is primarily a function of $\Delta \cdot \tan(\tau)$, trim reductions between the

bare hull and the propelled hull of 2 or 3 degrees cause 2 to 4 pounds of drag reduction. The column in Table 7 labeled ΔD is a computed estimate of the drag reduction due to the trim change. It is simply:

$$\Delta D = \Delta \tan(\tau - \tau_{bare})$$

and is useful for comparison to the drag increase caused by the operation of the waterjet.

Examination of the results in Tables 5 - 7 leads to the following observations.

- In the bollard condition, the measured net thrust D_m obtained from the drag balance is in excellent agreement with the gross thrust T_{gr} calculated from the momentum equation, thus providing confidence in the test data.
- The jet velocity, V_j , is essentially linearly dependent upon impeller shaft revolutions n , as follows:

  Bollard condition . . . . $V_j = 0.16n$.

  At test speed . . . . . $V_j = 0.18n$

  This observation is qualitatively in agreement with the results of Reference 1.
- At the model self-propulsion point ($D_m \simeq 0$), the thrust deduction $(1 - t) \simeq 0.75$.
- With the waterjet operative, the model trim angle τ is approximately 2-3deg less than the towed bare hull model trim angle τ_{bare} .

ENERGY ANALYSIS

An analysis through the same two control volumes using the energy equation was done to quantify losses in the system. This analysis was particularly helpful in making comparisons of model results to the design method (see the following section). The basic energy equation from Ref.4 is,

$$\frac{\delta Q_h}{\delta t} - \frac{\delta W_s}{\delta t} = \frac{\partial}{\partial t} \int_{cv} \rho e \, dV + \int_{cs} \left(\frac{P}{\rho} + e\right) \rho \vec{V} \, d\vec{A}$$

was simplified in the absence of the time rate of change of internal energy, e , within the control volume, and the absence of heat lost or gained, to an expression which relates losses in the control volume to the difference between the initial and final energy in the flow. A further simplification to this expression, that of omitting the potential energy term, gave an expression for each control volume:

$$\frac{P_o}{\gamma} + \frac{V_o^2}{2g} = \frac{P_i}{\gamma} + \frac{\beta_i V_i^2}{2g} + L_{cv1}$$

and

$$\frac{P_i}{\gamma} + \frac{\beta_i V_i^2}{2g} = \frac{P_j}{\gamma} + \frac{\beta_j V_j^2}{2g} - w_s + L_{cv2}$$

where losses are positive quantities. With the assumptions, and the model test data, the losses are the only unknowns in each equation. The specific physics of these losses are not known, but because there are two control volumes, the major components of the losses are likely to be:

L_{cv1} = Entrance Loss + Ramp Friction + Shaft Friction

L_{cv2} = Bend Loss + Transition Loss + Shaft and Strut Friction + Wall Friction

The shaft work term w_s was computed from the thrust measurement rather than the torque measurement so that the efficiency of energy transmission by the propeller is not involved; that is, $w_s = T/\gamma A_j$. Table 7 shows that both L_{cv1} and L_{cv2} are increasing approximately with the square of the flow rate in the bollard condition. However, in the testing with model velocity greater than zero, L_{cv1} decreases with the square of the flow rate while L_{cv2} increases with the flow rate. As in the momentum analysis, there is greater confidence in the sum of the two control volume parameters than in those of either alone. $L_{cv1} + L_{cv2}$ increases approximately linearly with flow rate.

COMPARISON OF MODEL TEST RESULTS WITH THE DESIGN METHOD CALCULATIONS

In addition to manipulating the model test data, the computer program contained expressions which computed energy losses through the waterjet in approximately the same way as was done in the design method.[5] The design method used a pipe flow technique to compute friction and form losses for the various parts of the duct, namely: entrance friction and bend, shaft, transition, bearing tube, struts, and casing. These were found by using a local Reynolds Number for a nominal flow rate of 60 cubic feet per second at the manned testcraft scale. Friction factors and equivalent lengths were found and the ratio of head loss to flow rate yielded a typical pipe flow "k" as a constant to multiply against flow, $\bar{Q}^2$. The design method also included a loss in the form of a modification on the energy available in the free stream. This was termed *ram recovery* and assumed that only 70% of the free stream flow energy $V_s^2/2g$ could be converted to jet energy. The result of these calculations was an energy equation which formed one side of an equilibrium flow condition, "Head Required." The other side was formed by "Head Available" and was generated by assumptions on the efficiency of power transmission. The expression for required head in the design method is written:

$$H_{Req} = 0.0112\bar{Q}^2 + 0.000766\bar{Q}^2 + 0.000101\bar{Q}^2 - 0.0109V_s^2$$

where the first term is the jet energy; the next two are loss terms for the entrance and ramp, and for the duct from inlet to jet; and the last is the free stream energy less 30%. For comparison with the energy analysis above, it is more convenient to write this equation in the form:

$$H_{Req} = \frac{V_j^2}{2g} + 0.001062V_j^2 + 0.000140V_j^2 - 0.7\,\frac{V_s^2}{2g} \quad .$$

So there are essentially two loss terms, $0.001202V_j^2$ and $0.3\,\frac{V_s^2}{2g}$. Since the former term is Reynolds Number dependent, it was calculated for every run using the model Reynolds Number based on an equivalent diameter and

the known velocity at the inlet plane:

$$Rn = \frac{0.269\ V_i}{1.05 \times 10^{-5}} \quad .$$

From this Rn, a friction factor, f , was found from a curve fit of the 0.0 relative roughness line of a Moody Diagram.[4] Then the ramp friction and bend loss were calculated. The design method indicates that this portion is 82% of the total friction and form losses, so these losses were taken as 1.22 times this portion, that is:

$$L_F = 1.22 \left(\frac{\ell}{d}\right) f \frac{V_i^2}{2g}$$

where ℓ/d is the equivalent length/diameter ratio which is the same for model and manned testcraft. The total losses by the design method are then L_F and $0.3\ V_m^2/2g$, which is in Table 7 as L_R.

L_F increases linearly with the square of the flow (i.e., V_i, V_j, or $\bar{Q}$), while L_R is constant for constant model speed, so that the sum of these values increases at approximately the same rate as the sum of L_{cv1} and L_{cv2}. At the bollard condition, the agreement between the calculated and measured losses is poor. However, at $V_m = 8.01$ ft/sec the measured values only exceed those calculated by 15%, and at the higher speeds and at 8.01 ft/sec with the wedge, the measured values are less than, and within 10% of, the calculated values. Additional analysis is required to represent the bollard condition in the design procedure of Reference 5.

Another way of comparing the design method to the model measurements is on the basis of efficiencies. The design method assumes a pump efficiency of 0.77 for the entire operating range, where

$$\eta_{pump} = \gamma \bar{Q} H / 550\ SHP \quad .$$

The model test version of η_{pump} is based on the torque-in (as shown in the beginning of the "Data Analysis" section) and these values tend to peak in the range of 0.63 to 0.67, approximately 15% lower, at J_D values of approximately 0.75 for the runs with V_m not equal to zero. It is believed that this lower value of measured pump efficiency can be attributed to the larger tip clearance and higher viscous drag coefficient of the

model waterjet. η_{prop}, which is listed for the model test, was not calculated for the design method equilibrium flow conditions. η_{oa} is different from the propulsive coefficient, P.C., found in the design method in that η_{oa} includes the effects of the waterjet system operation on the vehicle drag; that is, η_{oa} compares power-in to net thrust times vehicle speed, and P.C. compares power-in to gross thrust times vehicle speed. Reductions in vehicle drag due to reduction of trim angle have, in some conditions, caused T_{net} to slightly exceed T_{gr}, but in most conditions, T_{net} is less than T_{gr}, which would result in P.C. being too great an estimate of overall efficiency for this particular vehicle.

COMMENT ON THE 2 DEGREE WEDGE

The 2 degree wedge placed on the model bottom, aft of the transom made a change in bottom contour. The major effect of the wedge on performance is seen in Figures 3 and 4. The altered bottom contour reduced running trim angles and consequently reduced vehicle drag by approximately 5%. In the powered test resuts, data at 8.01 ft/sec for the with-and without-wedge conditions can be compared. The efficiencies are better for the with-wedge condition, but only by 2 to 3%. This is due to a reduction in losses, which in the higher thrust range are 20% lower for the with-wedge condition. So the benefit of the 2 degree wedge is to vehicle performance more than to the propulsion performance.

CONCLUDING REMARKS

Towing tests of a scale model of a waterjet testcraft have generated experimental data which, when analyzed, have yielded the following evaluation of the method used to design the simple, bottom-inlet waterjet system:

- Pump efficiency of the model waterjet was lower than the designed efficiency to a degree consistent with the proportionately larger tip clearance and higher viscous drag coefficient of the model impeller blades.
- There is reasonable agreement between design calculations of system losses and losses calculated using model test measurements in an energy equation, when the craft is in forward motion. The design method does not appear applicable in the bollard condition and further development is required.
- Thrust deduction at the model self-propulsion point is $(1-t) \simeq 0.75$.
- Running trim with the waterjet operating is 2-3 deg less than for the bare hull tests at the same speed.

REFERENCES

1. van Manen, J.D. and Oosterveld, M.W.C., "Analysis of Ducted-Propeller Design." SNAME *Transactions*, New York, 1966.

2. Prandtl, L. and Tietjens, O.G., *Applied Hydro- and Aeromechanics*. Dover Publications, New York, 1957.

3. Etter, R.J., Krishnamoorthy, V., and Scherer, J.O., "Model Testing of Waterjet Propelled Craft. *Proceedings* of the Nineteenth General Meeting of the American Towing Tank Conference. Ann Arbor Science Publishers, Inc., Ann Arbor, Michigan, 1981.

4. Streeter, Victor L. and Wylie, E. Benjamin, *Fluid Mechanics*. McGraw Hill Book Company, New York, 1975.

5. Roper, John K., "Development of Water-Jet Propulsion Unit." Davidson Laboratory Report 2328, March 1983.

TABLE 1. MODEL PARTICULARS

	Light Load	Heavy Load With and Without Wedge
Weight, lbs	39.99	49.55
LCG forward of transom, ft	0.86	1.03
Static transom draft, ft	0.35	0.41
Static trim, deg	2.6	2.7

WATERJET DETAILS

Jet Area, ft^2	0.0491
Inlet Area, ft^2	0.0755
Jet Diameter, ft	0.250
Propeller	DL #79 4-blade right hand
Propeller, P/D	1.0
Propeller Diameter, ft	0.242

TABLE 2. EHP RESULTS, LIGHT LOAD (4500 lbs)

LIGHT LOAD

SR	TEMP	RA
4.83	72.7	0.00000

RUNNO	VM	VS	RM	RS	EHP	TAU	HEVS	WAS
182	6.67	10.00	9.22	1038.	32.	9.64	0.22	80.
181	7.34	11.00	9.88	1112.	38.	11.60	0.38	74.
180	8.01	12.01	9.62	1083.	40.	13.18	0.65	60.
178	8.68	13.01	9.87	1112.	44.	13.90	0.83	50.
177	9.34	14.00	9.72	1093.	47.	13.69	0.97	46.
174	10.01	15.00	9.40	1053.	49.	13.18	1.11	44.
173	11.35	17.01	8.70	966.	50.	11.76	1.34	41.
175	12.67	19.00	8.06	884.	52.	10.34	1.42	40.
179	13.35	20.01	7.77	846.	52.	9.65	1.43	40.

SR	Scale Ratio
TEMP	Water Temperature, ^{o}F
RA	Roughness Allowance Coefficient
VM	Model Velocity, ft/sec
VS	Manned Testcraft Velocity, mph
RM	Model Resistance, lb
RS	Manned Testcraft Resistance, lb
EHP	Effective Horsepower
TAU	Trim, deg
HVS	Heave at CG, ft
WAS	Manned Testcraft Wetted Area, ft^2

TABLE 3. EHP RESULTS, HEAVY LOAD (5576 lbs)

FULL LOAD

SR	TEMP	RA
4.83	72.7	0.00000

RUNNO	VM	VS	RM	RS	EHP	TAU	HEVS	WAS
171	6.67	10.00	12.16	1374.	42.	9.09	0.16	95.
169	7.34	11.00	13.66	1546.	52.	11.36	0.30	84.
167	8.01	12.01	13.73	1554.	57.	13.64	0.59	70.
165	8.68	13.01	13.76	1560.	62.	15.15	0.85	55.
163	9.34	14.00	13.49	1526.	66.	15.37	1.04	51.
160	10.01	15.00	13.52	1527.	70.	15.13	1.22	49.
159	11.35	17.01	12.84	1430.	75.	13.82	1.50	57.
161	12.67	19.00	11.51	1281.	75.	12.05	1.64	42.
162	14.01	21.01	10.54	1160.	75.	10.58	1.68	41.
164	14.68	22.01	10.03	1096.	74.	9.87	1.71	40.
166	15.35	23.01	9.70	1055.	75.	9.26	1.71	39.
168	16.02	24.01	9.35	1012.	75.	8.70	1.72	38.
170	16.69	25.02	8.98	962.	74.	8.17	1.72	38.
172	17.34	25.99	8.70	925.	74.	7.69	1.72	38.

TABLE 4. EHP RESULTS, HEAVY LOAD (5576 lbs) WITH 2 DEGREE WEDGE

FULL LOAD WITH WEDGES

SR	TEMP	RA
4.83	72.7	0.00000

RUNNO	VM	VS	RM	RS	EHP	TAU	HEVS	WAS
157	6.67	10.00	12.81	1449.	44.	9.36	0.16	95.
153	8.01	12.01	13.95	1579.	58.	13.60	0.63	70.
151	8.68	13.01	13.79	1561.	62.	14.66	0.88	59.
149	9.34	14.00	13.49	1524.	66.	14.80	1.05	53.
146	10.01	15.00	13.16	1485.	68.	14.39	1.24	49.
145	11.35	17.01	12.16	1362.	71.	12.90	1.52	46.
147	12.67	19.00	10.98	1217.	71.	11.18	1.63	44.
150	14.67	21.99	9.54	1039.	70.	9.01	1.68	41.
152	15.34	22.99	9.22	999.	71.	8.42	1.68	40.
154	16.01	23.99	8.81	947.	70.	7.82	1.70	39.
156	16.68	25.00	8.49	906.	70.	7.28	1.68	38.
158	17.34	25.99	8.15	862.	69.	6.77	1.71	38.

Run #	V_m	τ	z	n	D_m	T	Q	V_j	P_i	P_j	D_{bare}	T_{bare}
113	0.00	2.78	0.001	20.20	1.07	0.87	0.040	3.18	13.25	8.87	0.00	2.78
114	0.00	2.75	0.002	30.40	2.42	1.80	0.076	4.76	3.79	8.97	0.00	2.75
115	0.00	2.74	0.001	38.60	3.85	2.84	0.114	6.04	-6.23	8.91	0.00	2.74
116	0.00	2.75	0.000	43.00	4.99	3.67	0.147	6.84	-13.75	8.95	0.00	2.75
117	0.00	2.71	0.003	50.00	6.85	4.98	0.193	8.13	-23.57	8.91	0.00	2.71
118	0.00	2.72	0.004	60.20	9.67	6.97	0.268	9.78	-43.78	3.09	0.00	2.72
119	0.00	2.66	0.005	73.00	15.19	10.83	0.420	12.30	-78.13	-2.21	0.00	2.66
120	0.00	2.66	0.005	83.70	19.99	14.19	0.554	13.83	-106.18	-2.34	0.00	2.66
121	0.00	2.62	0.006	93.00	24.39	17.00	0.678	15.21	-138.23	-2.04	0.00	2.62
72	8.01	11.21	0.043	42.00	-15.68	0.78	0.076	7.44	25.70	-2.22	-13.95	13.64
73	8.01	10.86	0.044	49.30	-14.41	2.03	0.126	8.81	18.77	-2.16	-13.95	13.64
74	8.01	10.54	0.028	59.50	-12.50	3.87	0.204	10.47	6.18	-2.22	-13.95	13.64
75	8.01	10.25	0.027	65.40	-10.87	5.35	0.258	11.89	-4.08	-7.61	-13.95	13.64
76	8.01	9.97	0.026	74.50	-8.35	7.60	0.349	13.37	-18.99	-7.64	-13.95	13.64
77	8.01	9.34	0.027	88.30	-3.61	11.67	0.518	15.90	-45.90	-13.54	-13.95	13.64
78	8.01	9.04	0.020	95.80	-1.33	13.90	0.612	17.17	-59.47	-13.29	-13.95	13.64
79	9.34	13.29	0.131	84.00	-5.47	9.34	0.431	14.93	-25.84	-7.81	-13.49	15.37
80	9.34	13.83	0.137	67.10	-10.63	4.83	0.249	12.17	5.51	-7.68	-13.49	15.37
81	9.34	13.66	0.136	75.00	-8.42	6.78	0.327	13.41	-7.96	-7.55	-13.49	15.37
82	9.34	12.70	0.115	93.30	-2.39	12.15	0.551	16.90	-41.49	-13.33	-13.49	15.37
83	9.34	11.89	0.103	136.50	3.04	16.85	0.753	19.28	-71.39	-13.16	-13.49	15.37
84	14.01	10.78	0.298	135.50	2.76	15.14	0.694	19.66	-14.83	-2.05	-10.54	10.58
85	15.35	9.68	0.307	139.00	2.72	15.26	0.716	20.04	-2.50	3.36	-9.70	9.26
124	8.01	10.75	0.038	42.10	-15.65	1.11	0.071	7.60	24.44	-2.45	-13.73	13.60
125	8.01	10.55	0.039	50.10	-14.31	2.40	0.124	9.04	17.69	-2.45	-13.73	13.60
126	8.01	10.53	0.039	59.70	-12.75	3.79	0.184	10.57	8.89	-7.52	-13.73	13.60
127	8.01	10.16	0.038	65.50	-10.69	5.46	0.254	11.96	-2.74	-7.99	-13.73	13.60
128	8.01	10.02	0.035	73.30	-8.47	7.36	0.332	13.48	-15.96	-8.07	-13.73	13.60
129	8.01	9.72	0.032	81.30	-5.83	9.54	0.422	15.04	-31.24	-13.26	-13.73	13.60
130	8.01	9.40	0.028	89.70	-2.86	12.04	0.532	16.51	-49.18	-13.46	-13.73	13.60
131	8.01	8.65	0.017	108.50	1.74	15.76	0.683	18.60	-77.37	-18.91	-13.73	13.60

TABLE 5. POWERED TEST DATA
(Runs 124-131 are with 2 degree wedge)

Run #	V_m	n	J_{fs}	J_d	$K_{\bar{Q}}$	K_H	K_T	K_Q	(1-t)	η_{oa}	η_{pump}	η_{prop}
113	0.00	20.2	0.000	0.651	0.495	0.359	0.321	0.0605	0.000	0.000	0.550	0.000
114	0.00	30.4	0.000	0.647	0.492	0.328	0.293	0.0511	0.000	0.000	0.591	0.000
115	0.00	38.6	0.000	0.646	0.491	0.320	0.286	0.0476	0.000	0.000	0.618	0.000
116	0.00	43.0	0.000	0.657	0.500	0.333	0.298	0.0494	0.000	0.000	0.631	0.000
117	0.00	50.0	0.000	0.672	0.511	0.335	0.300	0.0480	0.000	0.000	0.667	0.000
118	0.00	60.2	0.000	0.671	0.511	0.323	0.289	0.0460	0.000	0.000	0.672	0.000
119	0.00	73.0	0.000	0.696	0.529	0.341	0.305	0.0489	0.000	0.000	0.692	0.000
120	0.00	83.7	0.000	0.683	0.519	0.340	0.304	0.0491	0.000	0.000	0.674	0.000
121	0.00	93.0	0.000	0.676	0.514	0.330	0.295	0.0487	0.000	0.000	0.653	0.000
72	8.01	42.0	0.788	0.732	0.557	0.074	0.066	0.0266	0.885	-0.695	0.290	0.312
73	8.01	49.3	0.672	0.738	0.561	0.140	0.125	0.0323	0.887	-0.094	0.456	0.415
74	8.01	59.5	0.556	0.727	0.553	0.184	0.164	0.0358	0.880	0.152	0.531	0.407
75	8.01	65.4	0.506	0.751	0.571	0.210	0.188	0.0375	0.850	0.233	0.600	0.404
76	8.01	74.5	0.444	0.742	0.564	0.230	0.206	0.0391	0.840	0.274	0.621	0.372
77	8.01	88.3	0.375	0.744	0.566	0.251	0.225	0.0413	0.793	0.288	0.646	0.325
78	8.01	95.8	0.346	0.741	0.563	0.255	0.228	0.0414	0.747	0.275	0.649	0.303
79	9.34	84.0	0.459	0.734	0.558	0.222	0.199	0.0379	0.893	0.330	0.613	0.384
80	9.34	67.1	0.575	0.749	0.570	0.180	0.161	0.0344	0.895	0.255	0.560	0.430
81	9.34	75.0	0.515	0.739	0.562	0.203	0.181	0.0361	0.900	0.307	0.590	0.411
82	9.34	93.3	0.414	0.748	0.569	0.235	0.210	0.0393	0.808	0.321	0.635	0.351
83	9.34	136.5	0.283	0.584	0.444	0.152	0.136	0.0251	0.749	0.239	0.503	0.244
84	14.01	135.5	0.427	0.600	0.456	0.139	0.124	0.0235	0.962	0.315	0.504	0.359
85	15.35	139.0	0.456	0.596	0.453	0.133	0.119	0.0230	1.013	0.305	0.489	0.375
124	8.01	42.1	0.786	0.746	0.567	0.106	0.094	0.0249	0.866	-0.820	0.451	0.476
125	8.01	50.1	0.661	0.746	0.567	0.161	0.144	0.0308	0.864	-0.118	0.554	0.491
126	8.01	59.7	0.554	0.731	0.556	0.179	0.160	0.0321	0.845	0.114	0.580	0.440
127	8.01	65.5	0.505	0.755	0.574	0.214	0.191	0.0368	0.839	0.233	0.625	0.418
128	8.01	73.3	0.452	0.760	0.578	0.230	0.206	0.0384	0.810	0.275	0.649	0.386
129	8.01	81.3	0.407	0.764	0.581	0.242	0.217	0.0397	0.775	0.293	0.665	0.354
130	8.01	89.7	0.369	0.761	0.578	0.251	0.225	0.0411	0.746	0.290	0.663	0.322
131	8.01	108.5	0.305	0.709	0.539	0.225	0.201	0.0360	0.693	0.266	0.629	0.271

TABLE 6. POWERED TEST COEFFICIENTS
(Runs 124-131 are with 2 degree wedge)

Run #	V_m	n	$\bar{Q}$	T_{gr}	T_{net}	ΔD	F_{cv2}	F_{cv1}	F_{p2}	F_{p1}	F_{w2}	F_{w1}	L_{cv2}	L_{cv1}	L_F	L_R
113	0.00	20.20	0.156	1.05	1.07	0.00	0.40	0.66	0.57	-1.00	-1.04	1.66	0.25	-0.06	0.02	0.00
114	0.00	30.40	0.234	2.36	2.42	0.00	0.89	1.47	-0.15	-0.29	-0.76	1.76	0.28	0.01	0.05	0.00
115	0.00	38.60	0.296	3.79	3.85	0.00	1.43	2.36	-0.91	0.47	-0.50	1.89	0.32	0.07	0.08	0.00
116	0.00	43.00	0.336	4.86	4.99	0.00	1.83	3.03	-1.48	1.04	-0.36	1.99	0.36	0.12	0.10	0.00
117	0.00	50.00	0.399	6.87	6.85	0.00	2.59	4.28	-2.22	1.78	-0.18	2.50	0.44	0.15	0.13	0.00
118	0.00	60.20	0.480	9.95	9.67	0.00	3.75	6.20	-3.46	3.31	0.24	2.89	0.56	0.27	0.19	0.00
119	0.00	73.00	0.604	15.74	15.19	0.00	5.93	9.80	-5.79	5.90	0.90	3.90	0.79	0.44	0.28	0.00
120	0.00	83.70	0.679	19.89	19.99	0.00	7.50	12.39	-7.90	8.02	1.21	4.37	1.04	0.61	0.35	0.00
121	0.00	93.00	0.747	24.08	24.39	0.00	9.08	15.00	-10.34	10.44	2.41	4.56	1.03	0.85	0.41	0.00
72	8.01	42.00	0.365	0.08	-1.73	2.10	2.17	-1.52	2.05	-1.05	-0.65	-0.47	0.14	0.30	0.11	0.30
73	8.01	49.30	0.432	1.35	-0.46	2.40	3.04	-1.02	1.52	-0.30	-0.51	-0.72	0.21	0.27	0.15	0.30
74	8.01	59.50	0.514	3.41	1.45	2.68	4.30	-0.09	0.58	0.95	-0.15	-1.04	0.29	0.27	0.21	0.30
75	8.01	65.40	0.584	5.63	3.08	2.93	5.55	1.00	0.07	2.00	0.13	-1.01	0.38	0.24	0.26	0.30
76	8.01	74.50	0.656	8.39	5.60	3.18	7.01	2.40	-1.06	3.44	0.47	-1.04	0.49	0.24	0.33	0.30
77	8.01	88.30	0.781	14.17	10.34	3.73	9.92	5.47	-2.80	6.06	1.05	-0.60	0.74	0.19	0.45	0.30
78	8.01	95.80	0.843	17.57	12.62	3.99	11.57	7.32	-3.84	7.41	1.50	-0.09	0.82	0.13	0.51	0.30
79	9.34	84.00	0.733	9.90	8.02	1.80	8.74	2.49	-1.57	4.21	0.97	-1.72	0.51	0.39	0.40	0.41
80	9.34	67.10	0.597	4.57	2.86	1.33	5.81	-0.15	0.79	1.29	0.18	-1.44	0.29	0.36	0.28	0.41
81	9.34	75.00	0.658	6.77	5.07	1.48	7.05	0.91	-0.23	2.55	0.50	-1.64	0.39	0.39	0.33	0.41
82	9.34	93.30	0.830	14.67	11.10	2.31	11.20	4.98	-2.48	5.81	1.53	-0.84	0.63	0.23	0.50	0.41
83	9.34	136.50	0.947	21.51	16.53	3.01	14.58	8.65	-4.74	8.62	2.47	0.02	0.81	0.15	0.63	0.41
84	14.01	135.50	0.965	13.97	13.30	-0.17	15.16	1.43	-1.02	4.55	1.04	-3.12	0.83	0.77	0.65	0.92
85	15.35	139.00	0.984	12.47	12.42	-0.36	15.75	-0.35	-0.35	3.85	0.85	-4.20	0.83	1.07	0.68	1.10
124	8.01	42.10	0.373	0.21	-1.92	2.47	2.26	-1.48	1.97	-0.93	-0.82	-0.54	0.21	0.30	0.12	0.30
125	8.01	50.10	0.444	1.61	-0.58	2.64	3.21	-0.91	1.46	-0.18	-0.65	-0.73	0.28	0.26	0.16	0.30
126	8.01	59.70	0.519	3.55	0.98	2.65	4.38	-0.02	1.04	0.76	-0.45	-0.78	0.37	0.22	0.21	0.30
127	8.01	65.50	0.587	5.76	3.04	2.98	5.61	1.06	0.19	1.92	-0.03	-0.86	0.42	0.20	0.27	0.30
128	8.01	73.30	0.662	8.61	5.26	3.10	7.13	2.52	-0.81	3.24	0.57	-0.72	0.44	0.17	0.33	0.30
129	8.01	81.30	0.738	12.05	7.90	3.36	8.87	4.33	-1.71	4.75	1.04	-0.42	0.54	0.13	0.40	0.30
130	8.01	89.70	0.811	15.75	10.87	3.63	10.69	6.32	-3.05	6.46	1.70	-0.14	0.61	0.11	0.48	0.30
131	8.01	108.50	0.913	21.81	15.47	4.29	13.57	9.65	-4.91	9.14	2.73	0.51	0.71	0.09	0.59	0.30

TABLE 7. POWERED TEST ANALYSIS RESULTS
(Runs 124-131 are with 2 degree wedge)

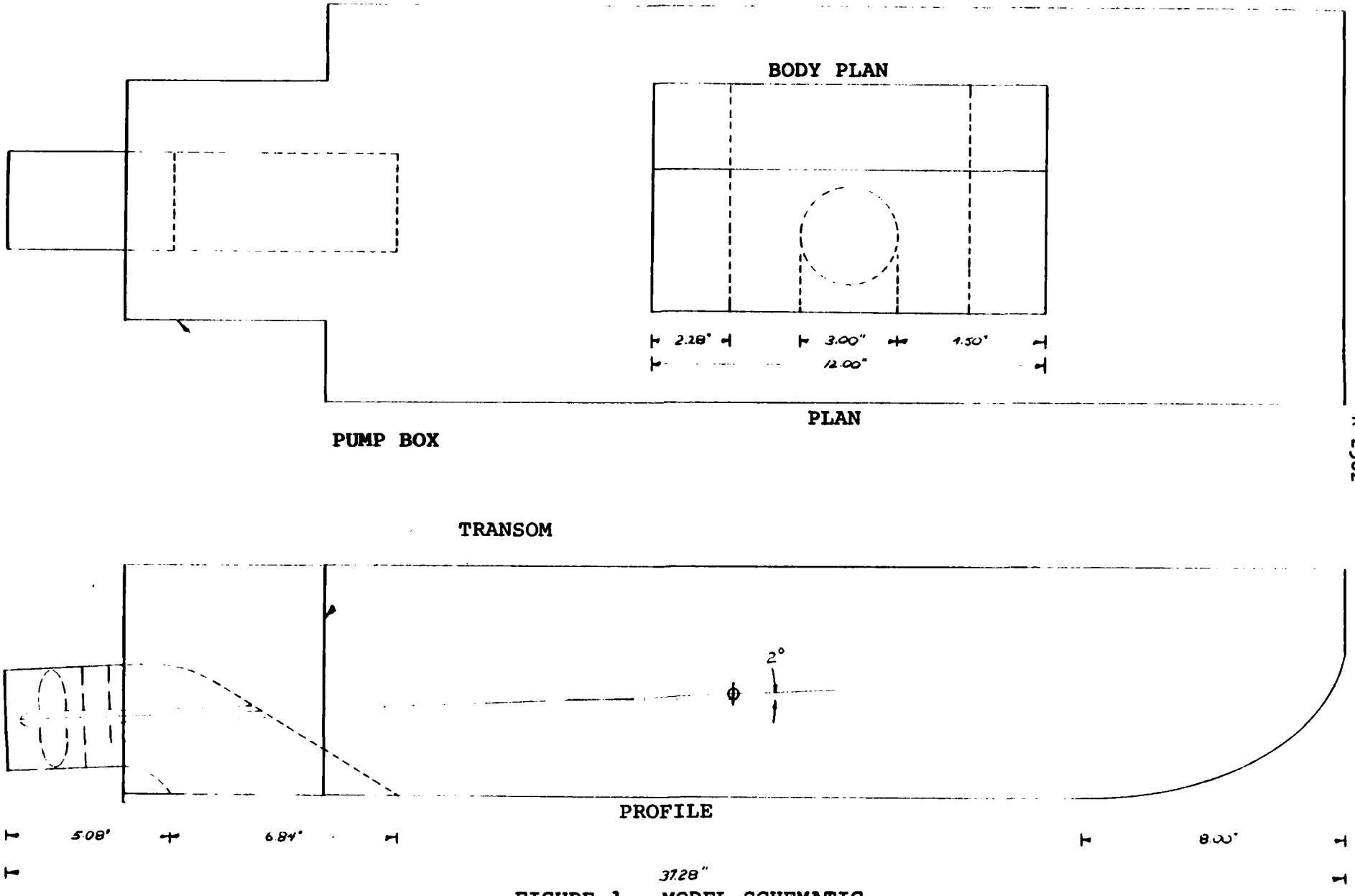

FIGURE 1. MODEL SCHEMATIC

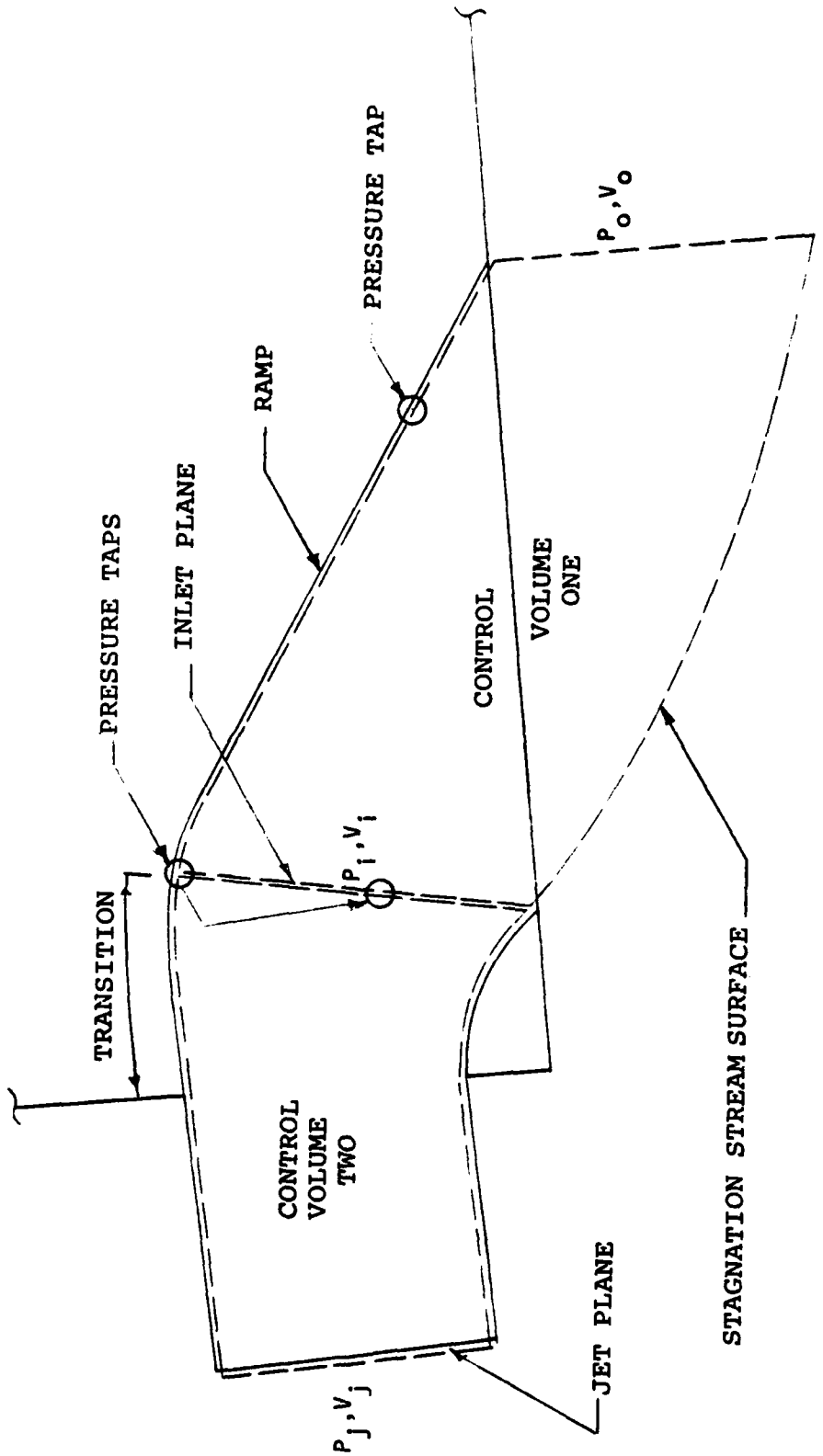

FIGURE 2. CONTROL VOLUMES

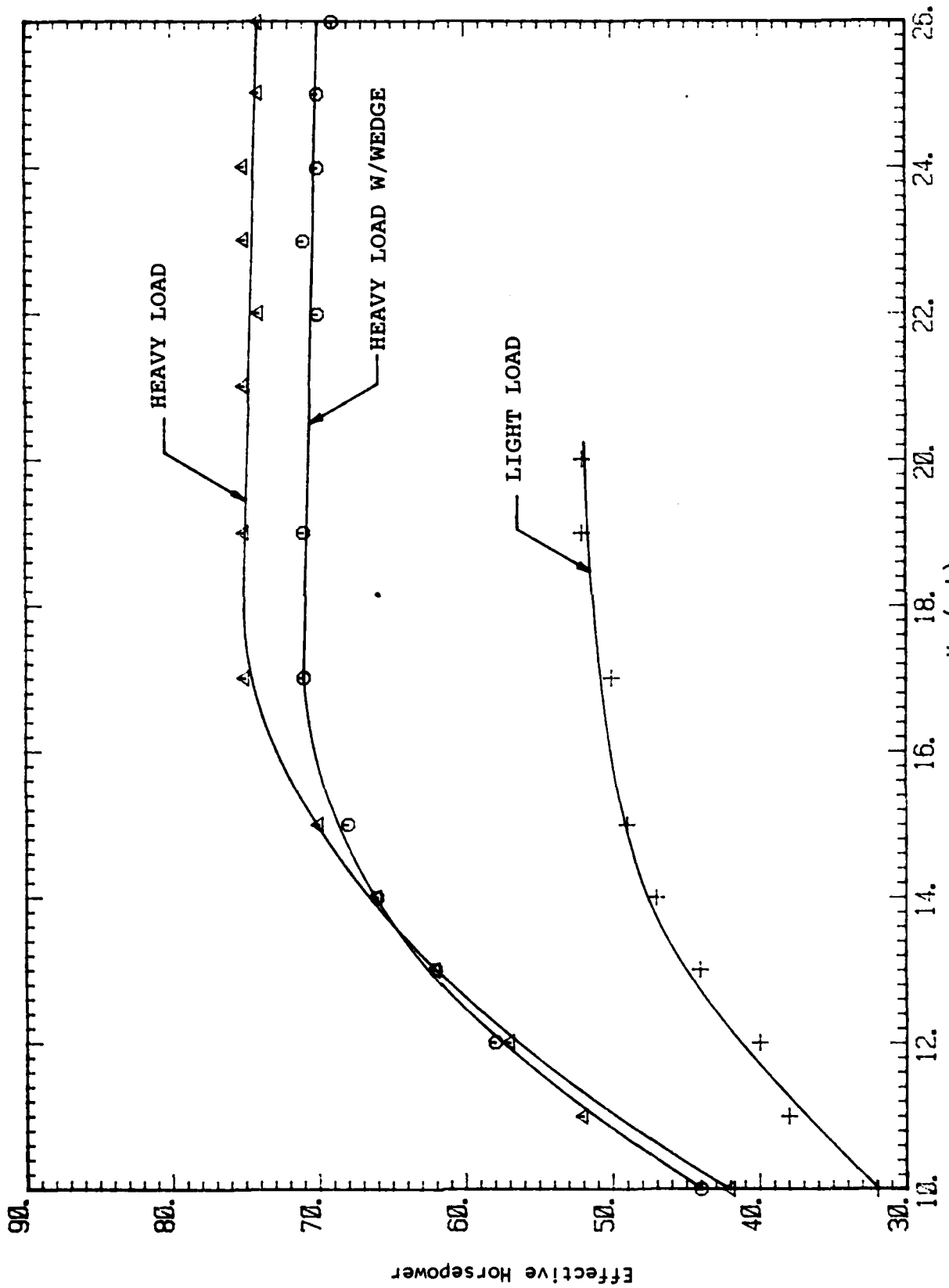

FIGURE 3. EFFECTIVE HORSEPOWER CURVES

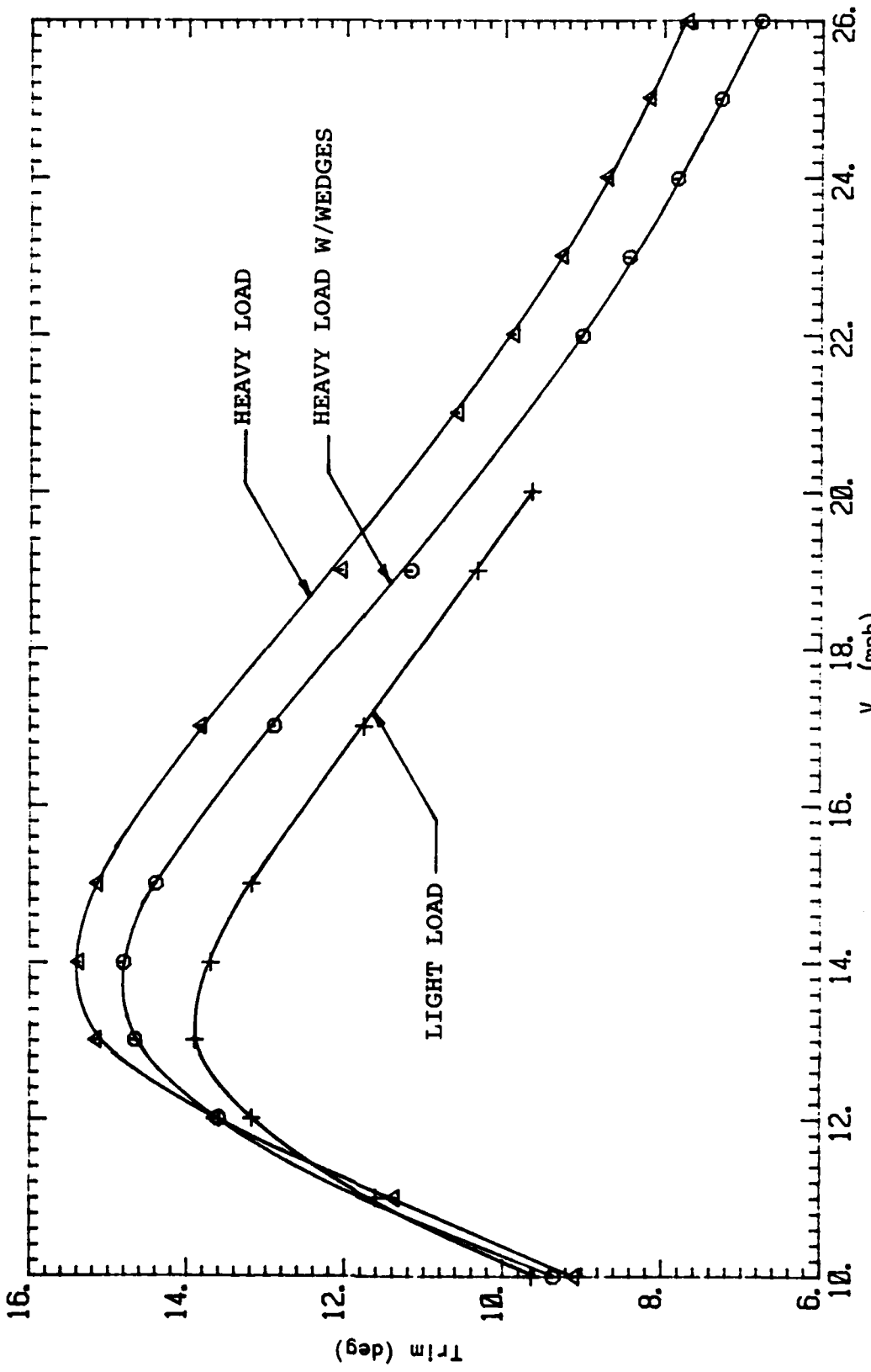

FIGURE 4. TRIM CURVES

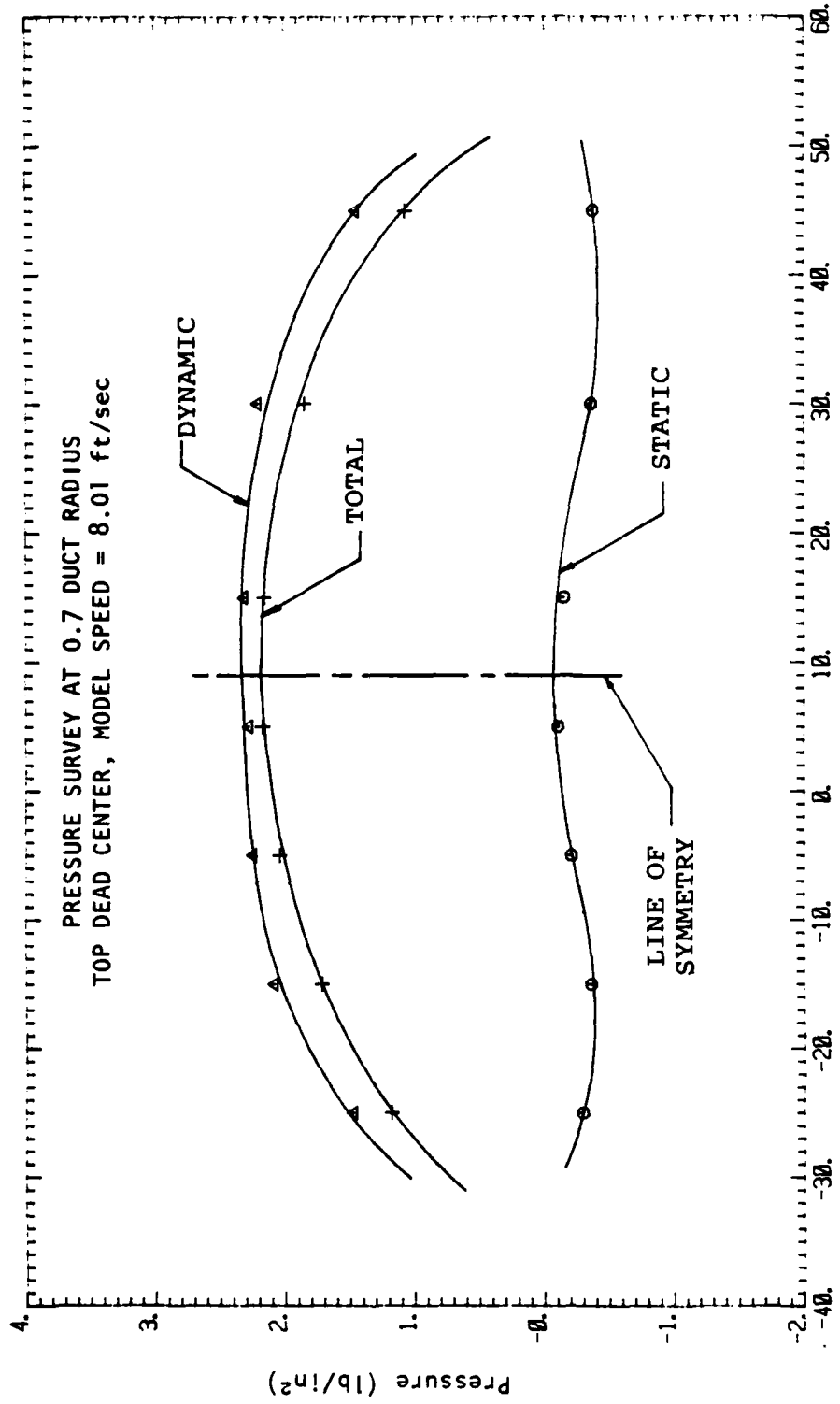

FIGURE 5. TANGENTIAL FLOW DETECTION

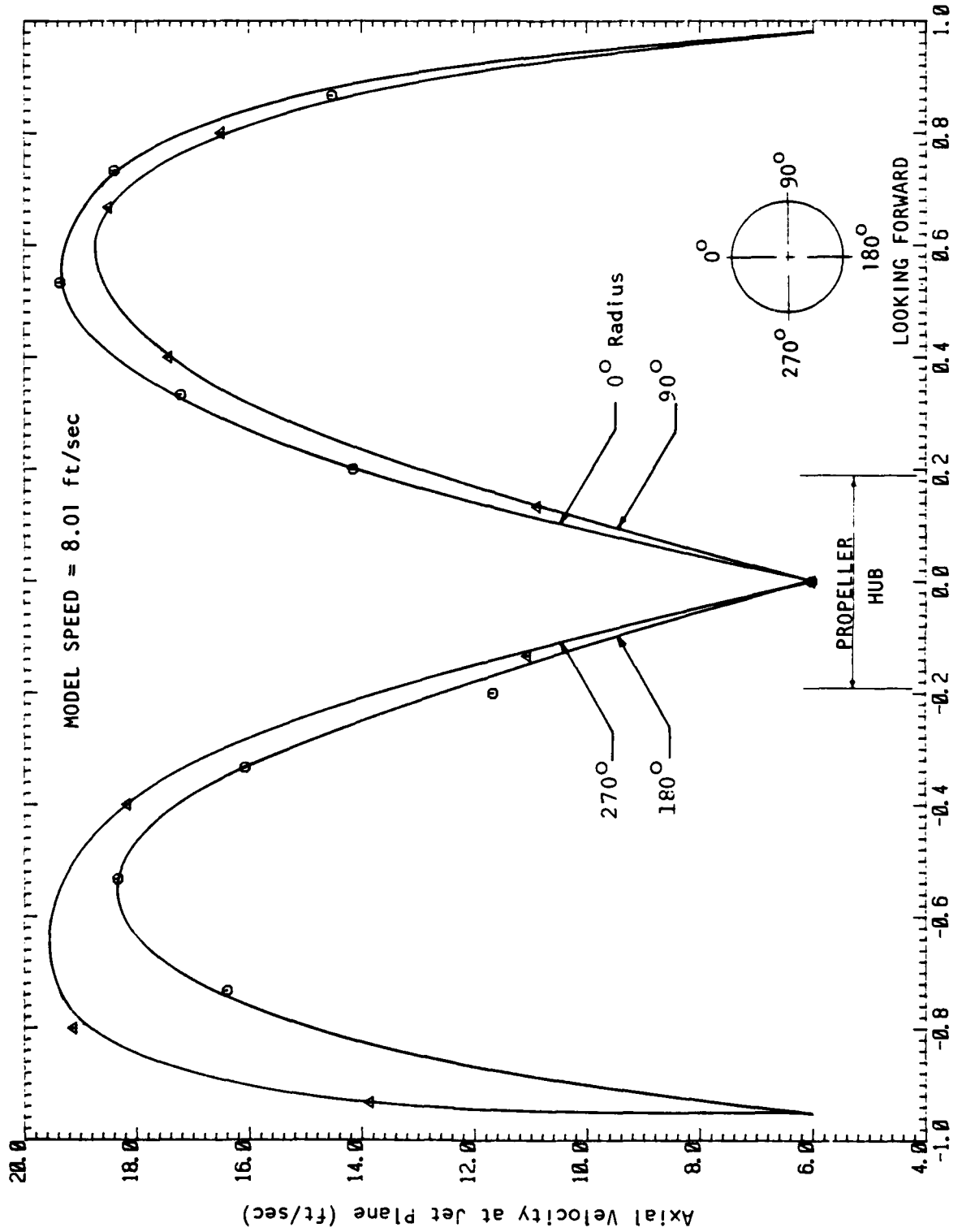

FIGURE 6. JET VELOCITY DISTRIBUTION

DISTRIBUTION LIST
(Contract N00167-82-K-0114)

Copies	
6	DAVID W. TAYLOR NAVAL SHIP RESEARCH AND DEVELOPMENT CENTER Bethesda, MD 20084 Attn: Code 1120
1	OFFICE OF NAVAL RESEARCH Branch Office Building 114, Section D 666 Summer Street Boston, MA 02210
1	OFFICE OF NAVAL RESEARCH Resident Representative 715 Broadway, 5th Floor New York, NY 10003
12	DEFENSE TECHNICAL INFORMATION CENTER Building 5, Cameron Station Alexandria, VA 22314